Available online at www.sciencedirect.com
SCIENCE DIRECT®
Journal of Organometallic Chemistry 674 (2003) 50–55
Journal of Organometallic Chemistry
www.elsevier.com/locate/jorganchem

Ligand influences on hydrogen migration in transition metal hydrido–carbyne complexes

Heiko Jacobsen *

KemKom, 1864 Burfield Ave., Ottawa, ON, Canada K1J 6T1

Received 14 February 2003; received in revised form 25 March 2003; accepted 27 March 2003

Abstract

Density Functional BP86 calculations are reported for the interconversion reactions of $WH(CH)(CO)(PH_3)_3$ and $WH(CH)(CO)_2(PH_3)_2$ to the corresponding five-coordinated carbene complexes $W(CH_2)(CO)(PH_3)_3$ and $W(CH_2)(CO)_2(PH_3)_2$, respectively. Transition states have been calculated to be 9.9 and 0.7 kcal mol^{-1} higher in energy than the carbynes. A comparison with the isoelectronic osmium system $OsHCl_2(CMe)(PH_3)_2$ with a transition state for interconversion 27.2 kcal mol^{-1} above the carbyne leads to the conclusion that additional π-acceptors competing with the carbyne or carbene ligand for back donation facilitate the interconversion reaction, whereas additional π-donors undergoing synergic push–pull interactions impede the interconversion reaction.

Keywords: Metal hydrido–carbyne complexes; Transition; Push–pull interactions

1. Introduction

We are dealing here with the interconversion of transition metal carbyne and carbene complexes by α-substituent migration (Scheme 1) [1].

A variety of factors govern the equilibrium between these two species, including the kind of transition metal M, the nature of the migrating group R, as well as the makeup of the ligand coordination sphere L_n. What looks like an elementary and straightforward organometallic reaction step still offers a number of surprising insights into ligand tuning of organometallic reaction sequences. An intriguing example has recently appeared in the literature. While the 1,2-hydrogen migration in an osmium hydrido carbyne complex does not appear to proceed in a unimolecular single step reaction [2,3], the observations reported for an *isoelectronic* tungsten hydrido carbyne complex point to the fact that an intramolecular α-hydride shift indeed constitutes a facile reaction step [4].

In order to elucidate this problem, presented are calculations for tungsten carbyne model compounds based on density functional theory (DFT) [5–7]. The increasing accessibility of fast DFT program packages offers an exceptional opportunity to learn about structures that might never reach detectable equilibrium, and DFT calculations as a complement to experimental work might provide impetus and stimulation towards chemically significant conclusions drawn not only from the experimentally observed, but also from the experimentally unobservable [8]. The calculations presented here may not only hold an answer to the above mentioned chemical conundrum, but may also aid in the understanding of the sensitive balance between five-coordinate carbene and six-coordinate carbyne complexes [9], and even be relevant in the clarification of activation of unsaturated carbon–carbon bonds with late transition metal hydrides [10].

2. Background

The tungsten carbyne fragment holds a variety of promising applications in organometallic chemistry, for example it provides access to cationic Lewis acidic

* Tel.: +1-613-2550058; fax: +1-613-8424831.
E-mail address: jacobsen@kemkom.com (H. Jacobsen).

0022-328X/03/$ - see front matter © 2003 Elsevier Science B.V. All rights reserved.
doi:10.1016/S0022-328X(03)00210-9

Scheme 1.

catalysts [11], as well as to activated transition metal hydrides [12]. In the latter context, the tungsten hydrido–carbyne complex $WH(CMes)(CO)(P(OMe)_3)_3$ (**1**) has recently been prepared, and its reactivity investigated [4].

When **1** is treated with the phosphorus donor $P(OMe)_3$ at −50 °C, no exchange of carbon monoxide with phosphine is observed. Instead, a new compound appears, identified as the carbene complex $W(CHMes)(CO)(P(OMe)_3)_4$ (**5**). Complexes **1** and **5** are at equilibrium; at low temperatures and large excess of the phosphorus donor formation of product **5** is favored, whereas at higher temperatures or smaller amounts of excess $P(OMe)_3$, the equilibrium lies on the side of the hydride complex **1**. Similarly, the reaction between carbon monoxide and **1** does not result in an insertion of CO into the metal hydride bond, but instead produces the carbene complex $W(CHMes)(CO)_2(P(OMe)_3)_3$ (**8**). However, complex **8** is not in equilibrium with **1**.

Careful experimental investigations suggest the following reaction sequence (Scheme 2). In complex **1**, the hydride and the carbyne ligand occupy positions *trans* to each other. Dissociation of one $P(OMe)_3$ ligand leads to a five-coordinated intermediate **2**. Re-association of a phosphine ligand or coordination of carbon monoxide results in hydrido–carbyne complexes **3** and **6**, with the hydride and the carbyne ligand now in *cis* position. In the next step, hydride migration onto the carbyne moiety takes place, leading to five-coordinated carbene fragments **4** and **7**, respectively. Coordination of another ligand molecule then completes the formation of complexes **5** and **8**. Since **5** is in equilibrium with **1**, all steps in the reaction sequence leading to the formation of **5** are at equilibrium as well. In contrast, during the formation of **8**, at least one of the steps discussed above is irreversible, or conversely represents a chemical equilibrium, which lies almost exclusively on the product side.

The reaction sequence presented above was further supported by DFT calculations on suitable model compounds [4]. However, while the calculations address energetics of the reaction steps involved in carbyne to carbene interconversion, kinetics for the 1,2-hydridogen shift are not considered, and no corresponding transition states are reported.

A different type of carbyne to carbene interconversion is reported by Caulton and co-workers [2,3]. $OsHCl_2(CEt)(P^iPr_3)_2$ (**9**) reacts with CO within 14 h at 0.036 M and 25 °C in dichloromethane to form $OsCl_2(CHEt)(CO)(P^iPr_3)_2$ (**10**) (Scheme 3).

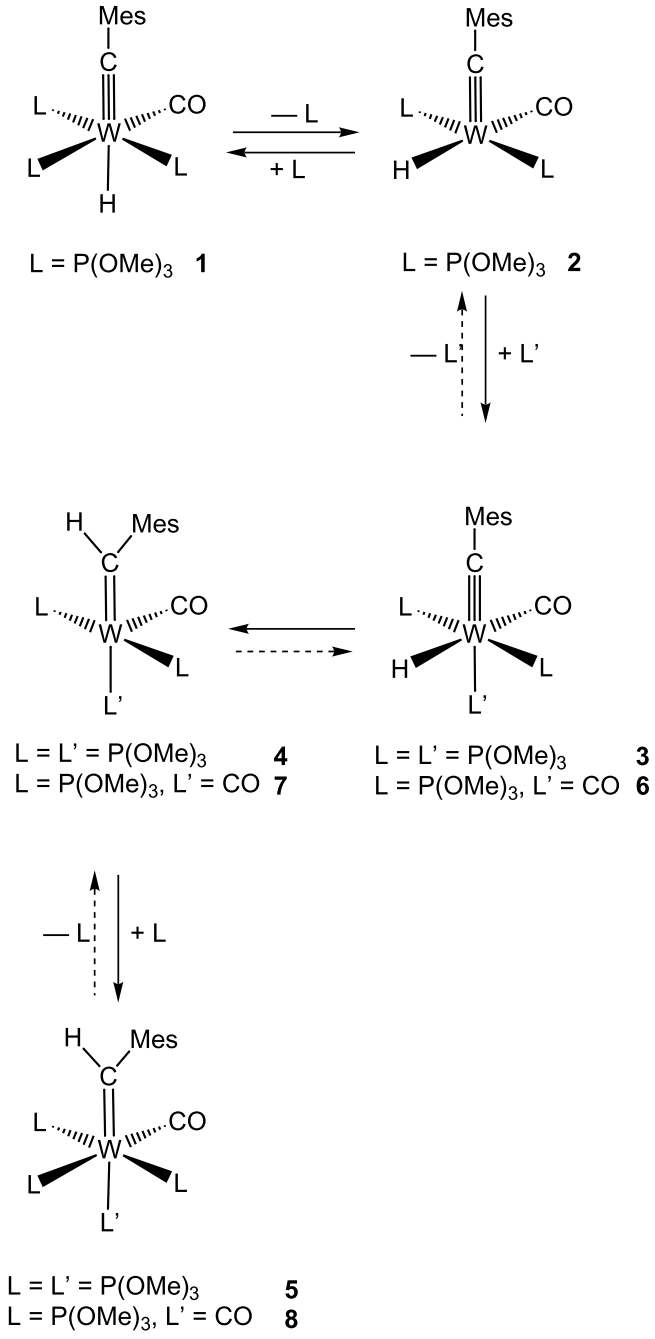

Scheme 2.

A stereochemistry with *trans* phosphines and *cis* chlorides is established by NMR spectroscopy. In contrast to the findings for the tungsten carbyne complex, a reaction of a rate as observed *cannot* occur by a mechanism in which an equilibrium amount of preformed unsaturated carbene $OsCl_2(CHEt)(P^iPr_3)_2$ (**11**) is attacked by CO. This conclusion is drawn from DFT calculations on the model compound $OsHCl_2(CMe)(PH_3)_2$ **IX** [3]. The energy of the optimized structure of the transition state **TSIII** for a unimolecular rearrangement between the hydride–carbyne complex **IX**

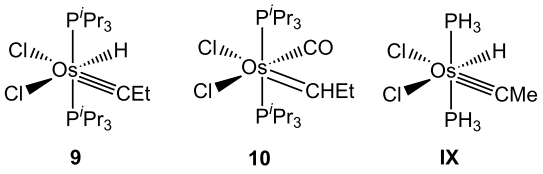

Scheme 3.

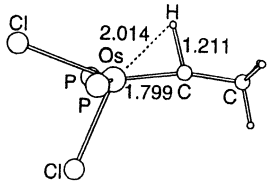

Fig. 1. Optimized transition state for the unimolecular rearrangement of $OsHCl_2(CCH_3)(PH3)_2$ into $OsCl_2(C(H)–CH_3)(PH_3)_2$ (reprinted with permission from Ref. [3], © 1998 American Chemical Society).

and the carbene complex $OsCl_2(CHMe)(PH_3)_2$ (**XI**) amounts to 27.2 kcal mol^{-1} above the carbyne, which is too large to be consistent with the observed reaction rate to form the carbonylation product. The optimized structure of **TSIII** is displayed in Fig. 1.

It is further concluded that the mechanism of this reaction must involve nucleophilic assistance of the hydride to carbyne–carbon migration; Os–CO bond making will lower the activation energy from its unimolecular value.

In line with presently evolving approaches in the integration of computational with experimental chemistry, which are especially successful in the field of transition metal hydride chemistry [13], calculations on the 1,2 hydride migration in tungsten carbyne complexes will now be presented. With density functional theory currently developing into a valuable research tool for the experimentally inclined chemist [14], it is hoped that basic concepts can be derived, which will explain the different reactivity of the tungsten and osmium complexes reported above.

3. Results and discussion

Geometries have been optimized for tungsten carbyne model compounds $WH(CH)(CO)(PH_3)_3$ (**III**) and $WH(CH)(CO)_2(PH_3)_2$ (**VI**), for the five-coordinated carbene intermediates $W(CH_2)(CO)(PH_3)_3$ (**IV**) and $W(CH_2)(CO)_2(PH_3)_2$ (**VII**), and corresponding transition states **TSI** and **TSII** have been located for the **III** → **IV** as well as **VI** → **VII** hydride migration, respectively (Scheme 4).

A prominent feature of the carbene intermediate is the agostic interaction between a carbene C–H bond and the transition metal center, characterized by W–H distances of 2.20 and 2.12 Å, elongated C–H bonds of 1.16 Å, and H–C–W angles of 87 and 83°, for model

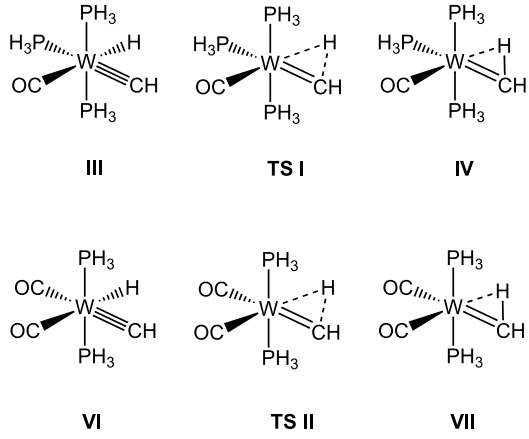

Scheme 4.

compounds **IV** and **VII**, respectively. This agostic interaction has already been observed and analyzed [4]; the analysis performed in the context of a neutron diffraction study of $W(CHMe)Cl_2(CO)(PMe_3)$ [15], has experimentally confirmed this structural feature.

In contrast to the tungsten complexes **IV** and **VII**, presumably no agostic interaction is calculated for the corresponding osmium carbene $OsCl_2(CHMe)(PH_3)_2$ (**XI**). The structure of **TSIII** (Fig. 1) suggests that the carbene ligand initially formed in **XI** is located in the Cl–Os–Cl plane. The reported calculations, however, indicate that the carbene ligand is rotated by 90°, and is located in the P–Os–P plane [3]. In this orientation, the electron donating chloride ligands can stabilize the electron accepting carbene ligand not only by metal mediated push–pull interaction, wherein π-donor and π-acceptor orbitals are coupled via a transition metal d-orbital, but also via vicinal σ-donation. Given the coordination geometry of complex **XI**, a double vicinal σ-donation becomes possible (Scheme 5). It is this particular orientation of the carbene ligand, which allows for a strong stabilizing interaction between chloride and carbene ligands, and which offers an explanation for the carbene system **XI** being energetically favored over the hydride–carbyne complex **IX** by 6.4 kcal mol^{-1} [3].

We will now turn to the geometries for transition states **TSI** and **TSII**, which are displayed in Fig. 2.

The transition states **TSI** and **TSII** have to be classified as early transition states, with long C–H separations for the forming bond, and values for W–

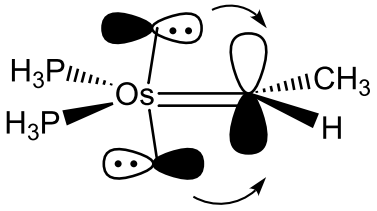

Scheme 5.

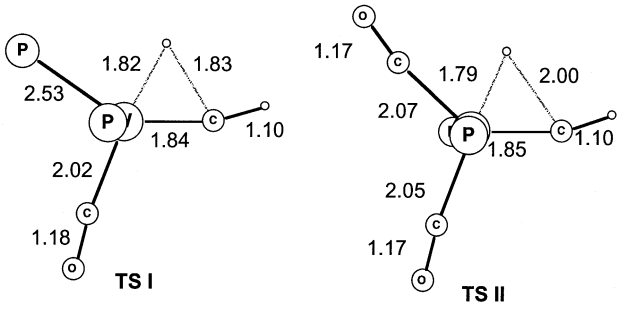

Fig. 2. Optimized transition state structures **TSI** and **TSII**.

H bond lengths only slightly longer or even slightly shorter than those for reactants **III** and **VI**, which amount to 1.80 and 1.81 Å, respectively. On the other side, transition state **TSIII** for the osmium system, as shown in Fig. 1, has to be classified as late transition state, with an Os–H elongated by about 0.4 Å compared to the corresponding osmium hydrido carbyne complex [3], and a short C–H separation indicates a preformed carbon–hydrogen bond. The two very different transition state structures for the tungsten and osmium carbyne systems provide a first indication as to the differences in chemical reactivity encountered.

Fig. 3 displays an energy profile for the α-hydride migration reactions **III**→**IV** as well as **VI**→**VII**. The energy of reactants **III** and **VI** is set to zero.

Transition state **TSI** is 9.9 kcal mol^{-1} higher in energy as compared to the corresponding reactant. This energy is significantly lower than the 27.2 kcal mol^{-1} reported for the osmium based **TSIII**, and is consistent with a unimolecular single step reaction, as previously proposed [4]. For **TSII**, an energetic increase of merely 0.7 kcal mol^{-1} above the reactant is observed. The energy profile presented in Fig. 3 provides a further explanation of why for the reaction of $WH(CMes)(CO)(P(OMe)_3)_3$ (**1**) with $P(OMe)_3$ an equilibrium is observed, but not for the reaction of **1** with CO. The activation barrier for the back reaction **IV**→**III** is 3.7 kcal mol^{-1} higher than that of the forward reaction, and both activation barriers are in the same order of magnitude. At higher temperatures, the equilibrium lies on the side of the reaction having the higher activation barrier. In contrast, the activation barrier for the back reaction **VII**→**VI** is 16.7 kcal mol^{-1} higher than that of the forward reaction, which provides an explanation as to why for the reaction between **1** and CO no experimentally observable equilibrium is reached.

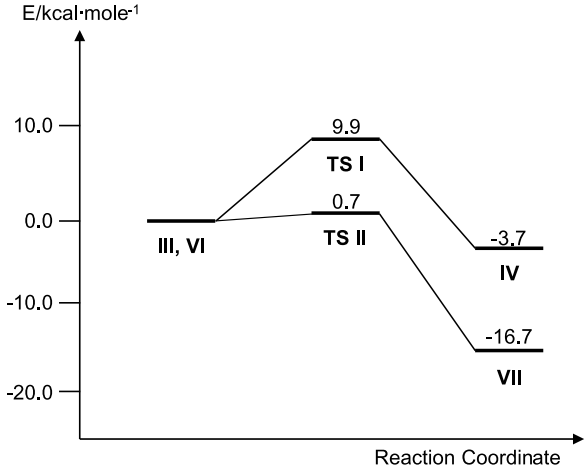

Fig. 3. Energy profiles for carbyne to carbene interconversion reactions **III**→**IV** and **VI**→**VII**.

Analysis of the bonding interactions for the tungsten and osmium systems explains the difference in calculated energy profiles for hydride migration reactions. When analyzing the bonding of a carbyne ligand, different descriptions are possible, based on either an anionic CR^- or on a cationic CR^+ model. According to a recent density functional analysis [16], the bonding in low-valent Fischer-type carbene complexes is best described by the cationic CR^+ model, which we will adopt for all isoelectronic species encountered in this work. In the tungsten as well as in the osmium case, we have a d^6-metal center, and the main bonding interactions for the carbyne CH^+ moiety are displayed in Scheme 6.

The carbyne ligand CH^+ acts as σ-donor as well as double π-acceptor. Hydride migration in carbyne hydrido complexes transforms the double π-accepting carbyne ligand into a single π-accepting carbene ligand. We also note that the hydride migration is not accompanied by a change of oxidation state of the transition metal center.

The bonding in the osmium system $OsHCl_2(CEt)(P^iPr_3)_2$ (**10**) is dominated by electron donating ligands, the carbyne moiety being the only strong electron acceptor. In particular, the chloride ligands not only act as σ-donors, but as π-donors as well, undergoing energetically favorable, synergetic π-interactions with the carbyne ligand. When hydride migration occurs, the π-accepting ability of this ligand is reduced, and the stabilizing push–pull interactions are

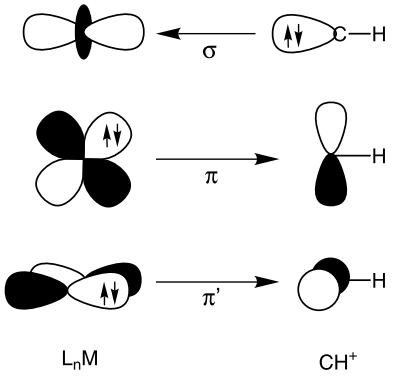

Scheme 6.

diminished. This causes an unfavorable energetic balance for hydride migration in the osmium system, manifested in a late transition state at high energy. Vicinal σ-donation renders the five-coordinated carbene system energetically favored over the six-coordinated carbine system, and additional coordination of another π-accepting CO ligand to the five-coordinated osmium carbene intermediate provides a further driving force for the carbonylation reaction of **10**.

A different scenario is observed for the intermediate $WH(CMes)(CO)(P(OMe)_3)_3$ (**4**). In this complex, no additional π-donor is present; instead, two π-acceptors compete for electron back donation from the transition metal center. When reducing the π-accepting power of the carbyne ligand, the electronic situation is more equally balanced, and as a consequence, the hydride migration is energetically favorable to a transition state requiring a substantially lower activation energy. This effect is even more pronounced in complex $WH(CMes)(CO)_2(P(OMe)_3)_2$ (**6**). Three π-acceptors are now competing for electron back donation, and the migration reaction transforming the strong double π-acceptor carbyne into an intermediate single π-acceptor carbene leads to a favorable and balanced electronic situation. It is for this reason that the five-coordinated carbene intermediate is energetically strongly favored over the carbyne complex **6**. As a consequence, the corresponding transition state for carbyne to carbene interconversion hardly poses an energetic barrier.

The bonding analysis presented above is supported by a charge analysis of reactants, products, and transition states. Values for a charge analysis are presented in Table 1.

We chose to perform a charge analysis using Voronoi deformation densities VDD, which affords a transparent interpretation based on the plausible notion of charge redistribution due to chemical bonding [17]. Therefore, VDD charges do not provide a good measure as to the anionic or cationic nature of a certain ligand, they do however provide a good measure of charge flow due to donation and back donation. Other charges obtained from other partition schemes are equally applicable to the problem, and lead to the same qualitative description.

For the CO ligands, we see a constant increase in negative charge, or an increase in back donation, when going from the carbyne complex via the transition state structure to the carbene compound. Similarly, the carbyne carbon gains positive charge when reaching the transition state, indicating reduced back donation. The additional increase in negative charge under product formation is due to the newly formed C–H bond. Clearly, the VDD charge analysis evidences reduced back donation to the carbene ligand as compared to the carbyne ligand, and an enhanced back donation to the carbonyl ligands in the carbene complex as compared to the carbyne complex.

4. Conclusion

Carbyne to carbene interconversion in transition metal hydrido carbyne complexes is governed by the π-bonding behavior of the auxiliary ligand framework. Since carbyne to carbene interconversion renders the changing ligand a weaker π-acceptor, additional π-acceptors competing with the carbyne or carbene ligand for back donation facilitate the interconversion reaction, whereas, additional π-donors undergoing synergic push–pull interactions impede the interconversion reaction. The presence of vicinal σ-donation might further favor a five-coordinated carbene system over the corresponding six-coordinated hydride carbyne complex.

5. Computational details

The density functional calculations utilized the ADF program package [18–21], release 2000.02. For the *n*s, *n*p, *n*d, and (*n*+1)s shells on W, a triple ζ-STO basis augmented by one (*n*+1)p function was employed

Table 1
Atomic charges (in a.u.) based on Voronoi deformation densities for tungsten carbyne complexes

	III	TSI	IV	VI	TSII	VII
C carbyne/carbene	−0.277	−0.227	−0.244	−0.253	−0.228	−0.237
C CO *trans* hydride	−0.022	−0.039	−0.080	0.012	0.007	−0.035
O CO *trans* hydride	−0.179	−0.187	−0.221	−0.158	−0.152	−0.183
C CO *trans* carbyne				0.073	0.018	−0.037
O CO *trans* carbyne				−0.112	−0.148	−0.170

(ADF database IV). The valence shell of main group elements was described by a double ζ-STO basis and one STO polarization function (ADF database III). The numerical integration grid was chosen in a way such that significant test integrals were evaluated with an accuracy of at least four significant digits for optimization of local minima, at least five significant digits for transition state searches, and at least six significant digits for frequency calculations. The self-consistent DF calculations were based on the local exchange-correlation potential of Vosko et al. [22], with self-consistent gradient corrections due to Becke [23] and Perdew [24] (BP86). Relativistic effects were included by using a quasi-relativistic approach [25]. Local minima were characterized by a spectrum of entirely real frequencies, whereas transition states were characterized by the presence of one imaginary frequency, corresponding to a displacement along a reaction coordinate.

6. Supplementary material

Cartesian coordinates and total bonding energies for optimized structures, as well as imaginary frequencies for transition states. Geometric representations for all optimized molecules are avaible from the author upon request.

Acknowledgements

M. Selbiger and Rechenzentrum der Universität Zürich for providing computational resources are gratefully acknowledged.

References

[1] K.G. Caulton, J. Organomet. Chem. 617 (2001) 56.
[2] G.J. Spivak, K.G. Caulton, Organometallics 17 (1998) 5260.
[3] G.J. Spivak, J.N. Coalter, M. Oliván, O. Eisenstein, K.G. Caulton, Organometallics 17 (1998) 999.
[4] E. Bannwart, H. Jacobsen, F. Furno, H. Berke, Organometallics 19 (2000) 3605.
[5] T. Ziegler, Chem. Rev. 91 (1991) 651.
[6] W. Kohn, A.D. Becke, R.G. Parr, J. Phys. Chem. 100 (1996) 12974.
[7] E.J. Baerends, O.V. Gritsenko, J. Phys. Chem. Sect. A 101 (1997) 5383.
[8] A.N. Vedernikov, K.G. Caulton, New J. Chem. 26 (2002) 1267.
[9] P. González-Herrero, B. Weberndörfer, K. Ilg, J. Wolf, H. Werner, Organometallics 20 (2001) 3672.
[10] A.V. Marchenko, H. Gérard, O. Eisenstein, K.G. Caulton, New J. Chem. 25 (2001) 1382.
[11] E. Bannwart, H. Jacobsen, R. Hübener, H.W. Schalle, H. Berke, J. Organomet. Chem. 622 (2001) 97.
[12] H. Jacobsen, H. Berke, J. Chem. Soc. Dalton Trans. (2002) 3117.
[13] F. Maseras, A. Lledos, E. Clot, O. Eisenstein, Chem. Rev. 100 (2000) 601.
[14] W. Koch, M.C. Holthausen, A Chemist's Guide to Density Functional Theory, Wiley-VCH, Weinheim, 2001.
[15] C.M. Bastos, K.S. Lee, M.A. Kjelsberg, A. Mayr, D. Van Engen, S.A. Koch, J.D. Franolic, W.T. Klooster, T.F. Koetzle, Inorg. Chim. Acta 279 (1998) 7.
[16] S.F. Vyboishchikov, G. Frenking, Chem. Eur. J. 4 (1998) 1439.
[17] F.M. Bickelhaupt, E.J. Baerends, Rev. Comp. Chem. 15 (2000) 1.
[18] E.J. Baerends, D.E. Ellis, P.E. Ros, Chem. Phys. 2 (1973) 41.
[19] L. Versluis, T. Ziegler, J. Chem. Phys. 88 (1988) 322.
[20] G. te Velde, E.J. Baerends, J. Comp. Phys. 99 (1992) 84.
[21] C. Fonseca Guerra, J.G. Snijders, G. te Velde, E.J. Baerends, Theor. Chem. Acc. 99 (1998) 391.
[22] S.J. Vosko, M. Wilk, M. Nusair, Can. J. Phys. 58 (1980) 1200.
[23] A. Becke, Phys. Rev. A38 (1988) 3098.
[24] J.P. Perdew, Phys. Rev. B33 (1986) 8822.
[25] T. Ziegler, V. Tschinke, E.J. Baerends, J.G. Snijders, W. Ravenek, J. Phys. Chem. 93 (1989) 3050.